Electronic Supplementary Material (ESI) for Soft Matter.

Assessing compressive elasticity and multi-responsive property of gelatin-containing weakly anionic copolymer gels via semi-IPN strategy

Sena CİFTBUDAK[a] and Nermin ORAKDOGEN[a*]

[a]Istanbul Technical University, Department of Chemistry, Soft Materials Research Laboratory, 34469, Maslak, Istanbul, Turkey.

*Correspondence to: Prof. Nermin Orakdogen (e-mail: *orakdogen@itu.edu.tr*), Phone: 0090-212-2853305

Structural characterization of gelatin and semi-IPN gels

The peak assignments for the FTIR spectra of gelatin-free copolymer GLN0-PAAm/ITA and semi-IPN GLNx-PAAm/ITA hydrogels has been shown in Table S1.

Table S1. The peak assignments for the FTIR spectra of gelatin-free copolymer GLN0-PAAm/ITA and semi-IPN GLNx-PAAm/ITA hydrogels.

	Peak Appearance Wavelength (cm^{-1})	
Characteristic Functional Group Assignments	**GLN free-Copolymer PAAm/ITA (cm^{-1})**	**Semi-IPN GLNx-PAAm/ITA (cm^{-1})**
carbonyl group (C=O) stretching of ($CONH_2$) of AAm	1648	1665
carbonyl group C=O of itaconic acid	1603	1611
NH2 stretching	3339	3342
N-H vibration	3184	3189
Aliphtic C−H stretching	2921	2928
$–CH_2–$ groups	1413	1421
symmetric stretching vibration of C-O-C	1122-875	1130-889
symmetric stretching vibrations of carboxyl groups.	1455	1456

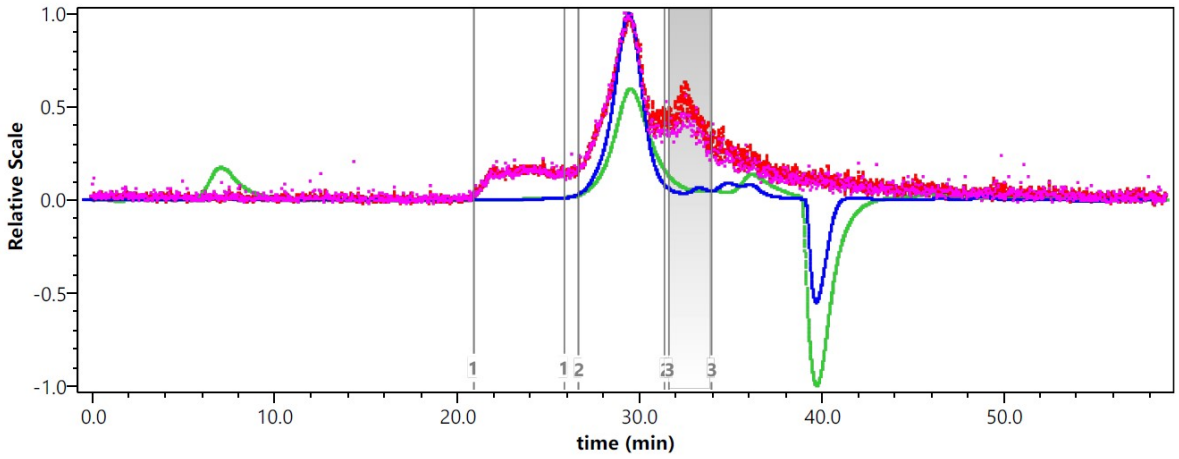

Figure S1. GPC trace of gelatin powder.

Stress-strain isotherms of semi-IPN hydrogels

Stress - strain isotherms of GLNx-PAAm/ITA semi-IPN hydrogels with AAm/ITA mol ratio of 98/2 after their preparation and after equilibrium swelling in water was presented in Figure S1. The GLN concentration of gels were indicated in the figure.

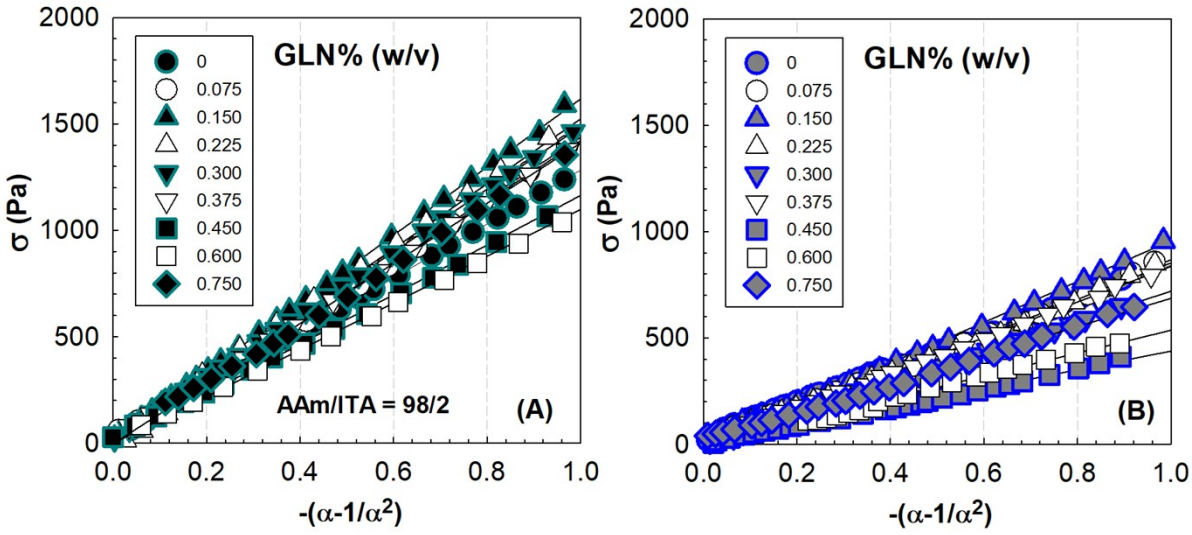

Figure S2. Stress - strain isotherms of GLNx-PAAm/ITA semi-IPN hydrogels with AAm/ITA mol ratio of 98/2 after their preparation (A) and after equilibrium swelling in water (B). The GLN concentration of gels were indicated in the figure.

Effect of GLN content on temperature-dependent swelling behavior of semi-IPN hydrogels

Figure S3 shows the equilibrium volume swelling ratio φ_V of GLNx-PAAm/ITA hydrogels at various swelling temperature as a function of the GLN content.

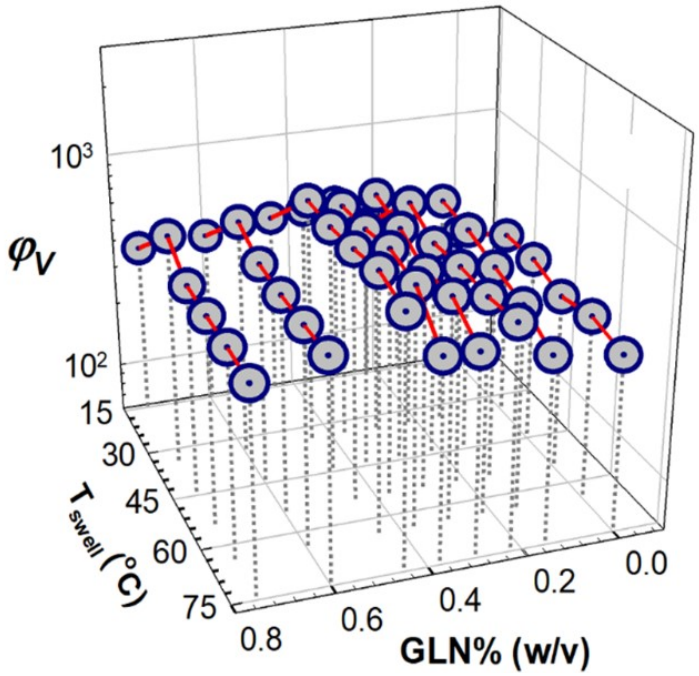

Figure S3. Equilibrium volume swelling ratio φ_V of GLNx-PAAm/ITA hydrogels at various swelling temperature as a function of the GLN content.

Effect of Hofmeister ions on the swelling

Figure S4 compares the equilibrium volume swelling ratio φ_V of semi-IPN GLNx-PAAm/ITA hydrogels as a function of the ionic strength of aqueous salt solutions of NaAc, $NaNO_3$ and NaSCN, respectively.

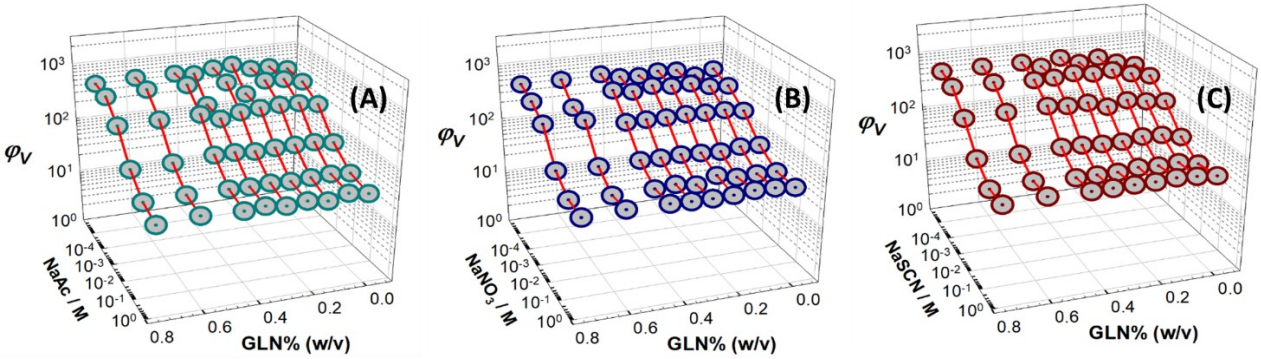

Figure S4. Equilibrium volume swelling ratio φ_V of semi-IPN GLNx-PAAm/ITA hydrogels as a function of the ionic strength of aqueous salt solutions of NaAc, $NaNO_3$ and NaSCN, respectively.

Adsorption properties of semi-IPN hydrogels

Figure S5 presents the time profiles of adsorption % of MB and MG dye for semi-IPN GLNx-PAAm/ITA hydrogels prepared at different GLN content as a function of contact time. Pseudo-first order kinetic model, Avrami model, Fractional-order model and Elovich model were further used to fit the adsorption data by using the following equations:

$$\frac{dq_t}{dt} = k_1(q_e - q_t), \quad \ln(q_e - q_t) = \ln q_e - k_1 t \tag{1a}$$

$$\ln\left[\ln\left(\frac{q_e}{q_e - q_t}\right)\right] = n_{Av} \ln k_{Av} + n_{Av} \ln t \tag{1b}$$

$$\ln q_t = \ln k_{fr} + n_{fr} \ln t \tag{1c}$$

$$q_t = \frac{1}{\beta}\ln t + \frac{1}{\beta}\ln(\alpha\beta) \tag{1d}$$

where k_1 (min^{-1}) is the pseudo-first-order rate constant. The equations and fittings of these models are given in Figure S6. From the slope and the intercept of a linear graph with negative slope from the plot of $\ln(q_e - q_t)$ against time t at different concentrations, in Figure S6, gives k_1 and $q_{e1,calc}$, respectively. Eq.(1b) express the linear form of Avrami kinetic model. k_{Av} is Avrami rate constant, and n_{Av} is the Avrami exponent of time related to the change in adsorption mechanism. k_{Av} and n_{Av} values were obtained from the intercept and slope of the plot of $\ln[\ln(q_e/(q_e - q_t))]$ against lnt. The linear form of Fractional power kinetic model is depicted by Eq.(1c), where k_{fr} and n_{fr} are the fractional kinetic constants obtained from the intercept and slope of the plot of $\ln q_t$ versus $\ln t$, respectively. If adsorption kinetic data fits well into power function model, n_{fr} is less than unity. Since the n_{fr} coefficients obtained from the Fractional model in Table 4 and Table S2 are less than 1, the adsorption of cationic dyes can be explained by the fractional model, which shows the complexity of the adsorption that may follow more than one pathway. The Elovich kinetic model in its linear form is expressed by Eq.(1d), where α is chemisorption rate constant and β is a constant related to the extent of surface coverage. The constants α and β given in Table 4 and Table S2 were calculated from the intercept and slope of the plot of q_t versus $\ln t$, respectively. For Elovich model, where the solid surface of the adsorbent is assumed to be energetically heterogeneous, β constants given in Table 4 increased with increased in GLN content.

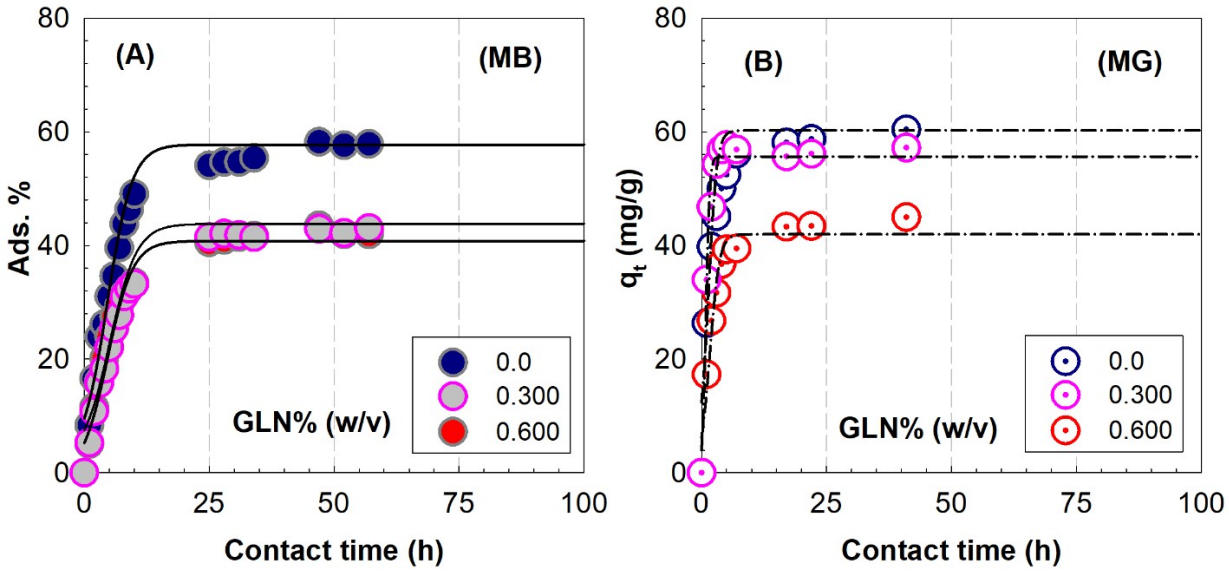

Figure S5. Time profiles of adsorption % of MB (A) and MG (B) dye for semi-IPN GLNx-PAAm/ITA hydrogels prepared at different GLN content as a function of contact time. Dye concentration: 5 mg/L.

Table S2. Kinetic parameters describing the adsorption of MG onto the semi-IPN adsorbents with different GLN content based on pseudo-first-order, pseudo-second-order, Avrami, Elovich, fractional power and intraparticle diffusion models. Initial MB concentration: 5 mg L^{-1}.

Pseudo-first order model			Elovich model		
GLN %(w/v)	$k_1 \times 10^{-1}$ (min^{-1})	R^2	α (mg/g min)	β (g/mg)	R^2
0	0.0613	0.9817	0.2413	0.4190	0.9872
0.300	0.1372	0.8522	0.3373	0.4921	0.9677
0.600	0.0681	0.9972	0.1059	0.5488	0.9979

Pseudo-second order model			Weber-Morris model			
GLN %(w/v)	$k_2 \times 10^{-3}$ (min^{-1})	R^2	$k_{initial}$ (mg g^{-1} $min^{-1/2}$)	R^2	$k_{later} \times 10^{-1}$ (mg g^{-1} $min^{-1/2}$)	R^2
0	1.6421	0.9998	0.3085	0.9848	1.0657	0.9911
0.300	2.0755	0.9996	0.4845	0.9965	2.2721	0.9979
0.600	7.5613	0.9996	0.5447	0.9966	2.5118	0.9233

Fractional power model				Avrami model		
GLN %(w/v)	n_{fr} (min^{-1})	k_{fr} (mg /g)	R^2	n_{Av}	$k_{Av} \times 10^{-1}$ (min^{-1})	R^2
0	0.3392	0.5910	0.9685	0.7828	0.0847	0.9949
0.300	0.4285	0.4953	0.9484	1.0715	0.1472	0.9875
0.600	0.5128	0.0893	0.9883	0.6168	0.0736	0.9418

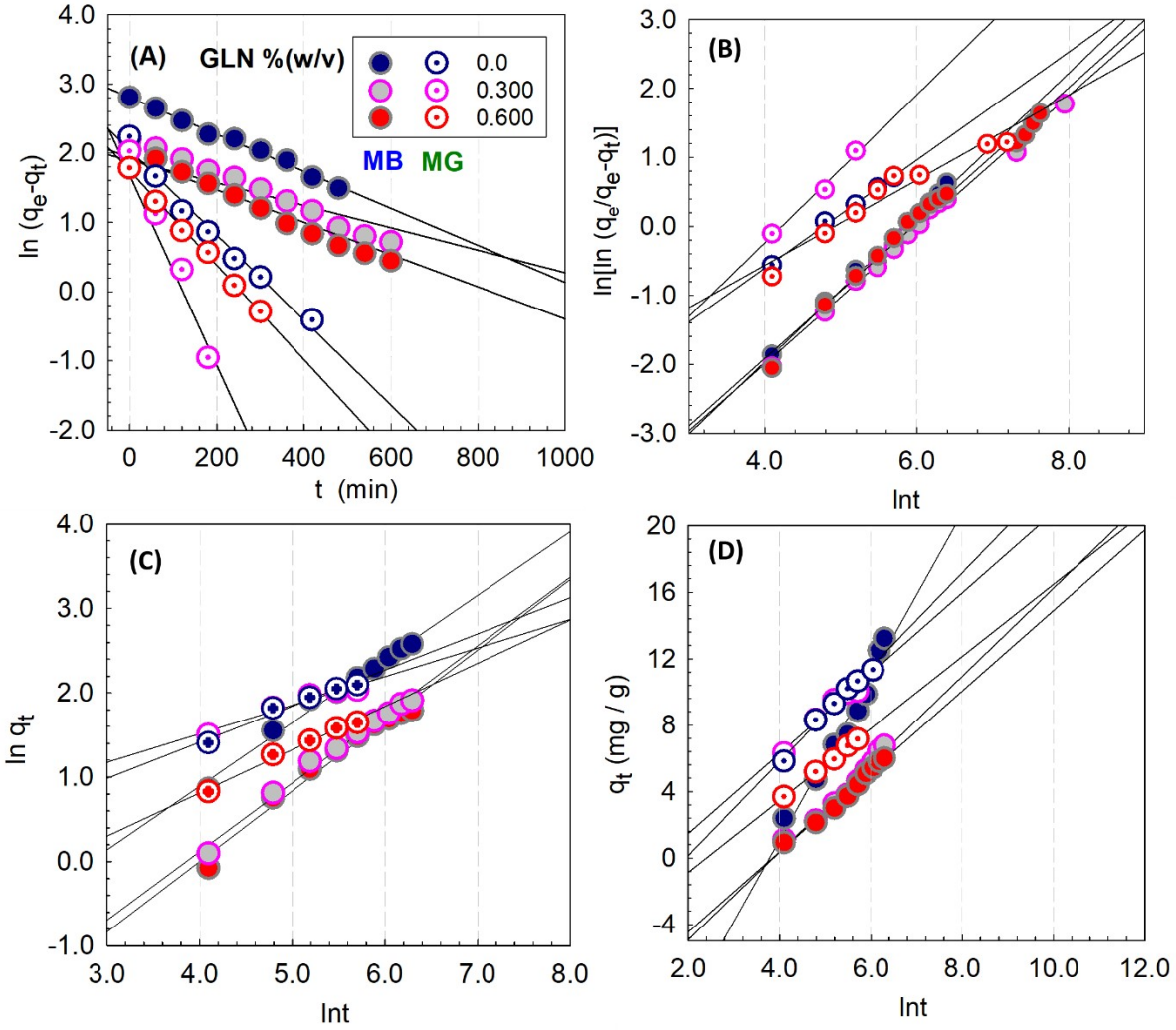

Figure S6. Adsorption kinetics of MB and MG onto the semi-IPNs based on the pseudo-first order kinetic model (A), Avrami kinetic model (B), Fractional model (C), and Elovich model (D). The solid line indicates the model-fit in the experimental data. Dye concentration: 5 mg/L.

Table S3. Thermodynamic parameters for adsorption of MB and MG dyes and adsorption capacity of semi-IPN GLNx-PAAm/ITA hydrogels prepared at different GLN content calculated from various kinetic models.

	Methylene Blue				Malachite Green			
GLN %(w/v)	Exp. q_e (mg/g)	Pseudo-first order $q_{e1,calc}$ (mg/g)	Pseudo-second order $q_{e2,calc}$ (mg/g)	ΔG^o (kJ/mol K)	Exp. q_e (mg/g)	Pseudo-first order $q_{e1,calc}$ (mg/g)	Pseudo-second order $q_{e2,calc}$ (mg/g)	ΔG^o (kJ/mol K)
0	16.51	16.78	17.84	-4.537	9.378	7.730	9.613	-4.650
0.300	9.006	6.652	9.948	-2.287	7.580	5.365	7.610	-3.930
0.600	7.743	6.9153	8.418	-1.865	5.959	5.721	6.148	-2.711

The Langmuir, Freundlich, Temkin and Dubinin-Radushkevich (D-R) isotherm model are given as:

$$\frac{C_e}{q_e} = \frac{1}{q_{\max} K_L} + \frac{C_e}{q_{\max}} \quad \text{and} \quad R_L = \frac{1}{1 + K_L C_o} \tag{2a}$$

$$\ln q_e = \ln K_F + (1/n) \ln C_e \tag{2b}$$

$$q_e = B_T \ln K_T + B_T \ln C_e \quad \text{and} \quad B_T = \frac{RT}{b_T} \tag{2c}$$

$$\ln q_e = \ln q_{\max} - \beta \varepsilon^2 \quad ; \quad \varepsilon = RT \ln(1 + \frac{1}{C_e}) \quad \text{and} \quad E = \frac{1}{(-2\beta)^{1/2}} \tag{2d}$$

where $q_{\max}$ (mg g^{-1}), is the maximum adsorption capacity of the adsorbent, K_L (L/mg) is Langmuir adsorption constant, R_L is separation factor. The R_L value shows that the adsorption process is irreversible for $R_L = 0$, is favorable for $0 < R_L < 1$, linear for $R_L = 1$ or unfavorable for $R_L > 1$. According to Freundlich isotherm model given by Eq. (2b), K_F (mg/g)(mg/L)$^{-1/n}$ is Freundlich isotherm constant and n is adsorption intensity. Temkin isotherm can be modeled using Eq.(2c) with K_T (L/mg) is Temkin isotherm equilibrium binding constant, and b_T (J/mol) is Temkin isotherm constants related to heat of adsorption. Temkin isotherm model assumes that the heat of adsorption of all molecules decreases to their maximum bond energy with increasing coverage of the adsorbent surface. The main advantage of Temkin isotherm is that it allows the evaluation of the heat of the adsorption: if the constant b_T is positive, the adsorption process would be exothermic. For D-R isotherm model given by Eq.(2d), ε (J/mol) is the potential of Polanyi and β is D-R isotherm constant (mol^2 / J^2). This model assumes that the filling of micropores varies according to the adsorption capacity and the free enthalpy of adsorption changes by the degree of pore filling.